Data-Driven 3-D Tactile Cues With Intermediate Soft Interfaces Toward Training Needle Insertions

Ruijie Tang, Shilong Yao, Long Bai, *Graduate Student Member, IEEE*, Hong Yan, *Fellow, IEEE*, Max Q.-H. Meng, *Fellow, IEEE*, and Hongliang Ren, *Senior Member, IEEE*

***Abstract*—During the training of medical operators, forming muscle memory through repetitions is a routine path. Needle insertion is a fundamental skill for all medical staff. However, such training courses often require human resources at a relatively high cost. Therefore, a needle insertion simulator for large-scale deployment and practical training is expected. In this article, we design a passive, compliant force estimator that is low-cost, easily fabricated, and commonly demanded by needle insertion simulators. A triaxial decoupling force sensor design comprises commercial force-sensing resistors (FSRs), soft silicon materials, and a 3-D-printed connector for force decoupling. The total cost of the sensor and fabrication process is less than 5 USD. To achieve the prediction of a 3-D force profile when the corresponding medical tasks are performed, we propose and compare two data-driven estimators, including least-square (LS) regression and feedforward neural networks (FNNs). We demonstrate that FNN models outperformed the LS model regarding devised corresponding evaluation metrics. The predicted accuracy of the FNN is above 90%, while the LS has a lower average accuracy of 78.02%. Finally, we test the performance of a pretrained model on different angle gaps (15°, 30°). The force profiles of the 15° angle gap present relatively large fluctuations compared to reference with average accuracy at 84.36%. The test on the 30° angle gap has an error at 35.28%, which also shows randomness deviations from standard profiles. Therefore, the force information with a 15° or 30° angle gap can warn the trainer that an angle deviation exists from the standard setting.**

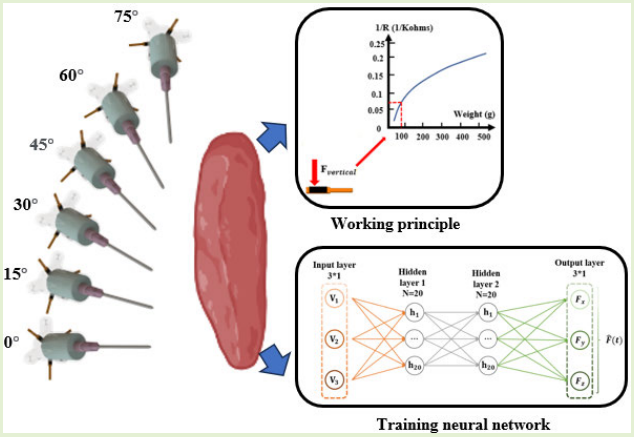

***Index Terms*—3D tactile sensor, data-driven, machine learning, needle insertion, simulator.**

I. Introduction

IN MEDICAL healthcare, training medical operators, including trainee nurses and surgeons, is crucial for the safety of patients, as medical errors can be the reason for death as well [1], [2]. Therefore, the comprehensive practical courses provide trainees with prior experience in the corresponding surgical procedure [3], [4]. In such courses, simulators can be an effective way for students to become familiar with standard medical operations. A steeper learning curve for trainees can be obtained. Besides, flexible training using a simulator that can avoid experienced clinicians' direct supervision is especially suitable for situations where human resources are insufficient.

Needle insertion, as shown in Fig. 1, is used in medical applications including retrobulbar anesthesia, punctures of pericardial effusions, biopsies, and percutaneous dilatational tracheostomy [5], [6], [7], [8]. Researchers investigate various methods, including positioning mechanisms [9], trajectory prediction and tracking [10], [11], and deep reinforcement learning [12] to reduce placement errors during needle insertion. However, for junior clinicians, it is likely that delicate body tissue, such as vessels and nerves, can be hurt if the

Manuscript received 1 December 2023; accepted 4 January 2024. Date of publication 23 January 2024; date of current version 29 February 2024. This work was supported in part by the Hong Kong Research Grants Council (RGC) Research Impact Fund (RIF) under Grant R4020-22, in part by the Collaborative Research Fund (CRF) under Grant C4026-21GF, in part by the General Research Fund (GRF) under Grant 14203323, in part by NSFC/RGC Joint Research Scheme under Grant N_CUHK420/22 and Grant GRS 3110167, in part by the Shenzhen-Hong Kong-Macau Technology Research Program (Type C) Shenzhen Science and Technology Innovation Committee (STIC) under Grant SGDX20210823103535014 and Grant 202108233000303, and in part by the Guangdong Basic and Applied Basic Research Foundation (GBABF) under Grant 2021B1515120035. The associate editor coordinating the review of this article and approving it for publication was Dr. Theerawit Wilaiprasitporn. *(Ruijie Tang and Shilong Yao contributed equally to this work.) (Corresponding authors: Max Q.-H. Meng; Hongliang Ren.)*

Please see the Acknowledgment section of this article for the author affiliations.

Digital Object Identifier 10.1109/JSEN.2024.3354289

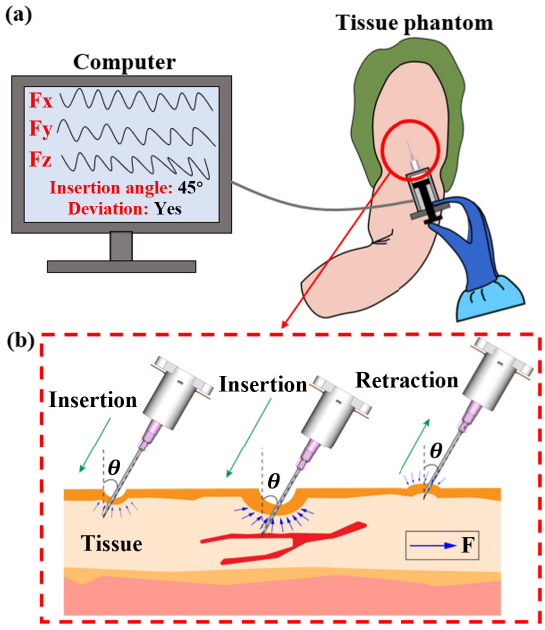

Fig. 1. (a) Demonstration of the needle insertion simulator integrated with proposed force estimator design. (b) Illustration of the needle insertion process: interacting with soft tissue. When the needle is inserted into the soft tissue at insertion certain angle, the deformable tissues can result in the reaction force acting on the needle. At the end of the retraction process, deformable tissue is lifted, which causes a downward force.

insertion angle is wrong or the force is too large. As needle insertion is a common and basic skill for nurses and surgeons, repeated training with effective feedback is required in needle insertion simulators. Fig. 1 also illustrates that 3-D-force profiles during the insertion process can be used in simulators to inform the trainer that they are in the acceptable range of insertion angle and the magnitude of insertion force. Therefore, effective force feedback on needle tips can benefit the training procedure of the simulator. The current experimental data show that inhomogeneous tool–tissue contacts are inevitable and expected. Then, obtaining the magnitude and direction of 3-D forces can assist the operator in reducing the deformation effect between needle and tissue [13].

Previous studies have investigated the direct force measurement system during needle insertion. Commercial sensors such as the ATI Nano series are widely used in clinical trials due to their high precision and quick response [14]. In the simulator platform, the key hardware setup is to mount such commercial sensors on the needle [15], [16], [17]. Nevertheless, the cost of such a device can be as high as 5000 USD. Thus, researchers investigated strain gauges integrated with specially designed shaped structures to replace the relatively expensive commercial device [18]. Piezoelectric sensors made of piezoelectric ceramics (PZT) and polyvinylidene fluoride (PVDF) materials are other options for needle insertion application. Despite their large force measurement range and small sizes, the accuracy is limited by the signal drifting caused by temperature variation and charge leakage [19]. Optical sensors such as fiber Bragg grating (FBG) are widely used in high-precision applications, including retinal vein cannulation and retrobulbar anesthesia [20]. To compensate for the effect of temperature, FBG sensors rely on expensive and complicated optical signal processing. The contact force sensor uses optoelectronic sensors and a disk-like sensor mechanical structure toward a flexible manipulator for minimally invasive surgery [21]. A novel data-driven paradigm proposed by Sefati et al. [22] including uncalibrated FBG sensors and related deep neural networks (DNNs) and temporal neural networks (TNNs) was used for sensing in surgical continuum manipulator. Besides, a general and convenient tactile cues paradigm is required for different novel bio-inspired needle designs [23].

Besides, soft materials are embedded in force-sensing systems in some medical applications for safety reasons. However, due to the nonlinearity and hysteresis, there are challenges in calibrating and controlling such compliant structures. To overcome the limitations, machine-learning methods have been implemented in soft tactile sensors for contact localization and force prediction [24]. Embedded soft materials are used for tactile sensing with established relationship modeling between light reflection and deformation [25]. The comparison between mathematical models and machine-learning estimators for soft sensors was studied in [26], and a recurrent neural network (RNN)-based sensing framework was proposed.

Thus, estimating 3-D force information with low hysteresis and low cost is crucial for prevalent needle insertion simulators. In this work, we design a low-cost 3-D-force estimator with intermediate soft interfaces as force conduction. We also implement a data-driven algorithm to predict force profiles during the needle insertion process toward different penetrating angles. To be specific, our main contributions include the following.

1) We design a novel soft material embedded force estimator to achieve 3-D sensing. The tripod-like structure is designed and 3-D-printed as a connector for force decoupling. The whole manufacturing process is designed in an integrated approach which is aimed at fixing the soft materials, the connector, and the needle.
2) We propose a novel data-driven paradigm for the needle insertion process. The inputs from the voltages of three piezoresistive sensors are fed to a data-driven framework for measuring tip force when interacting with tissues. The comparison study between the linear method (least-square (LS) regression) and hypernonlinear method feed-forward neural network (FNN) is carried out under different insertion angles. Based on the accuracy tests, we selected an FNN as a further validation data-driven framework. The overall accuracy of the FNN framework is above 90%, while the LS method fails to predict forces for most cases.
3) We carry out the tests of the FNN model with different insertion angle gaps. The force profiles with $\pm 15^\circ$ gap present relatively large fluctuations while can predict the trends of the reference curve. The force curves with $\pm 30^\circ$ gap show the unexpected large deviations from reference forces. Therefore, such features in force profiles can be used in needle insertion simulators to inform the trainees that the needle will correct the insertion angle to the ideal setting.

II. Mechanical Design and the Fabrication Process of the Force Estimator

A. Triaxial Decoupling Structure Design

Except for accuracy and sensitivity, there are relatively high requirements for the size of the force estimator for in vivo medical operations. The size of the estimator can limit the number of force dimensions as well. Tang et al. [27] designed a rigid cross structure that can be used to sense the decoupled triaxial force. Still, the diameter of the proposed structure is too large, which is unsuitable for interaction with human tissue during the needle insertion process [27].

The force-sensing resistor (FSR) is a low-cost, high-sensitivity flexible sensor widely used for normal pressure measurement. This small-scale FSR rapidly decreases its resistance value when the applied pressure increases. Besides, it can obtain a more obvious reading change by connecting a series of resistances.

The design contains three 2.5-mm-wide FSRs (Shenzhen LEGACT Technology Company Ltd., RP-W2.5-L15.5), a needle, a 3-D-printed connector, and a 3-D-printed base with a 14-mm diameter and 20-mm length base as shown in Fig. 2. The design fixes the needle with the connector and aligns its end with the FSRs. When the needle is inserted into the tissue, it generates a force in three directions through the devised connector structure. The force transmission in three directions of the tip will be carried out by the connection position at the end of the part. The embedded soft materials are pressed and squeezed to achieve the final stage of force transmission. The corresponding relationship of the force in the X-, Y-, Z-direction can be decoupled from the contact force between the axes in the connector and the FSRs. The voltage value is defined as the output through the FSR conversion circuit. This design enables the fabrication of the estimator in the most compact size, reaching a diameter of 14 mm. The design uses three FSRs worth 0.53 USD, allowing repeatable manufacturing at a meager cost and disposable medical devices. The 3-D-printed parts cost 4.2 USD, and the total cost to fabricate the estimator is less than 5 USD.

B. Integrated Fabricated Method

The reliability and stability of the estimator must be considered. Ecoflex[1] 00-30 is a highly durable soft silicone material that can transmit force without plastic deformation and can be used as an intermediate medium for 3-D-printed connectors and force estimators. Here, we use a one-piece molding method to fix the estimator, the connector, and the needle through Ecoflex[1] 00-30 to obtain a stable force coupling relationship. The fabrication process is shown in Fig. 3. After assembling and positioning the components, pour Ecoflex 0030 into the cavity. It is important to note that a preloaded weight of 50 g should be added during the curing process. The purpose of the preloaded weight is to increase the sensing range of the sensor, allowing the readings to appear even with forces of a few grams. In Fig. 4(b), when the applied force is below a certain threshold, it is difficult for the resistance to exhibit significant changes. This characteristic curve can also be investigated through static load experiments by placing loads of 10, 20, and 100 g on an FSR with a soft interface. When a 10-g load is applied, there is no significant change in the readings. With a 20-g load, there is a sudden spike in the readings. When a 100-g load is applied, the readings stabilize within certain fluctuations. Therefore, a preloaded weight from 20 to 100 g is reasonable, and we select 50 g. When the Ecoflex[1] 00-30 is cured, a mold is added under the connector. When the curing is completed, the lower mold can be removed to obtain an injectable cavity, which can also be adapted to broader medical applications.

The curing process requires first positioning the FSR in the center of the base groove, where the outer shell is waterproof. Then, we placed the 3-D-printed connector on the bottom cylindrical mold to ensure that the connector and the estimator were aligned with a 2-mm gap. The distance can result in better surface contact making the transmitted forces more accurate after the silicone cures. Thus, it can ensure the consistency of properties during repeated manufacturing. After that, the Ecoflex[1] 00-30 silicon is poured and cured for 8 h to obtain an estimator with stable performance. The holes of its base can be well fixed at the end of the UR5 robotic arm. The reserved orifice can be well connected between the needle and the syringe and can be used as a disposable device.

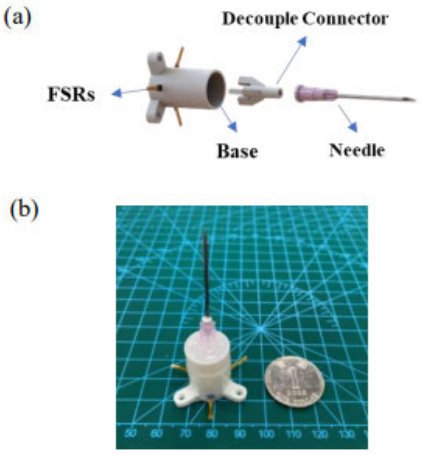

Fig. 2. (a) Components of proposed novel estimators include the base holder, FSRs, and a connector for the base and the needle. (b) Prototype estimator compared to the coin scale.

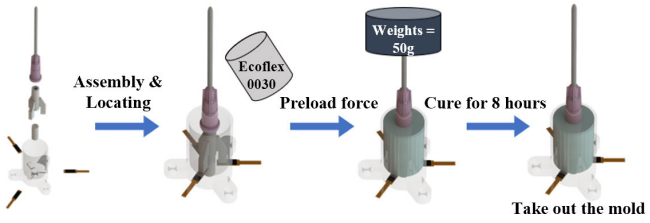

Fig. 3. Fabrication process of the proposed estimator design: the first step is to assemble all the parts and position the connector in the center of FSRs; the second step is to pour the Ecoflex[1] 00-30 into the mold; the third step is to place the initial weight (50 g) by piercing through the needle; the fourth step is to cure the Ecoflex[1] 00-30 and take out the mold.

[1]Registered trademark.

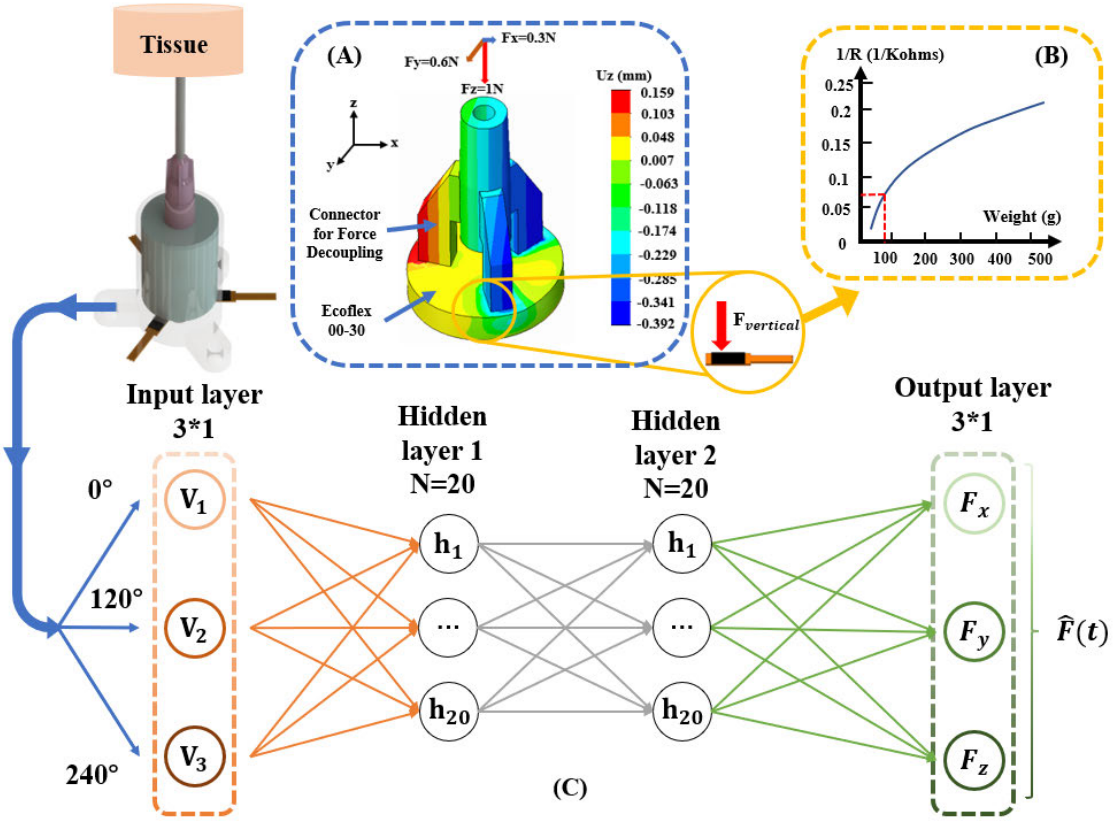

Fig. 4. Working principle of the force estimator and architecture of the FNN model. (a) FEA results of the connector and soft interfaces. (b) Relationship between exerted force and resistance. (c) Input layer contains three inputs from FSRs. The inputs are three voltage variations caused by normal pressure transmitted through the tripod structure and embedded soft materials. The relationship between pressure (g) and the reciprocal resistance of FSR is captured by a nonlinear curve. There are two hidden layers with 20 neurons in the serial. The reference forces are used in the output layer for training.

C. Working Principle of the Force Estimator

To demonstrate the working principle of the designed estimator, we perform the finite-element analysis (FEA) in SolidWorks 2021 to show how the intermediate soft interfaces conduct the force to three FSRs. As the hardness of the material of the connector is high, direct contact between the connector and FSR can be insensitive. Therefore, the soft interfaces assist the force transmission and improve the sensitivity of the designed estimators. Young's modulus of Ecoflex[1] 00-30 is set to 1.38 MPa, and the bottom of embedded soft materials is also fixed. Fig. 4(a) presents the results of FEA. Under an external force ($F_x = 0.3$ N, $F_y = 0.6$ N, and $F_z = 1$ N), the displacements on the Z-direction of soft interfaces for three corresponding FSRs places are -0.392, -0.229, and 0.159 mm, respectively. Besides, it shows that one deformation mode corresponds to a certain external 3-D force. Therefore, the decoupling of 3-D force can be achieved through data-driven methods. Fig. 4(b) shows the nonlinear curve of estimator resistance and the exerted force. It is worth noting that when the force approaches 0 N, the estimator fails to show variations in resistance, so we embed the soft materials to make the defined working area in the middle of the curve. This is useful for the situation at the end of the retraction process. When the lifted-up tissue causes the reaction force in the opposite direction (Fig. 1), readings from FSRs can change in a small range at the left side of the initial point.

III. Data-Driven Method Design and Implementation

We employ two data-driven algorithms, the LS regression method and the FNN, to predict the magnitudes of forces in the X-, Y-, and Z-directions.

A. LS Regression Method

To consider the linear transformation relationship between voltages and forces as follows:

$$\begin{bmatrix} F_x & F_y & F_z \end{bmatrix} = C \begin{bmatrix} v_1 & v_2 & v_3 \end{bmatrix} \tag{1}$$

where F_x, F_y, and F_z are 3-D force, and v_i is the corresponding voltage collected from pressure-sensing resistor (PSR) sensors. C represents the unknown calibration matrix. Therefore, the constructive relation of output voltage signals (V) and tip contact forces (F) is defined by the calibration matrix (C). Matrix C can be obtained from the LS regression as follows:

$$C = F\, V^T \left(V V^T\right)^{-1}. \tag{2}$$

The dataset is divided into a training set and a validation set, with 85% and 15% of the data, respectively.

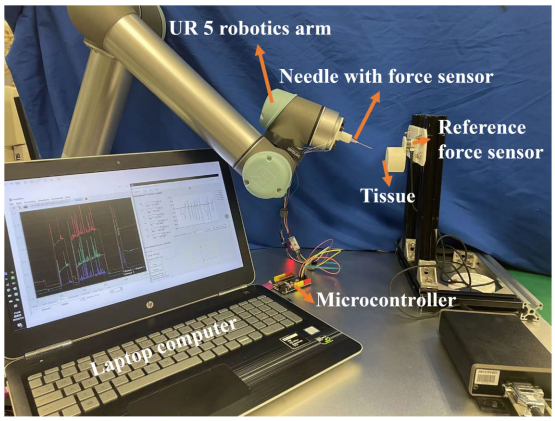

Fig. 5. Experimental setup for data collection of needle insertion.

B. Feed-Forward Neural Networks

The FNN is a typical artificial neural network containing only input, hidden, and output layers. Compared to a recurrent network, the framework has no cycle element. For the implementation of our model, the overall architecture of the neural network is shown in Fig. 4(c). The input voltages are from three evenly distributed FSRs where the gap is set to 120°. A series–parallel architecture is created with two input variables: voltage signals and reference forces. The signal vector $v = [v_1, v_2, v_3]$ represents three voltage outputs of the FSR unit. The reference force vector is represented as $F_r = [F_x, F_y, F_z]$. The advantage of a series–parallel structure is that input accuracy to FNN is improved. The division of training data (11 224 points) follows the setup as 85% for training, 5% for validation, and 10% for testing. After the training, we implemented the model to process the new dataset (12 546 points).

IV. Experimental Setup

Based on the framework of the sensing system, we will first obtain adequate data to train the interconnected network or regression test. Then, the experimental setup is designed as shown in Fig. 5. A 6-DoF robotic manipulator (UR5) performs the insertion task. The needle with the designed soft force estimator is attached to the robotic arm, and 3-DoF voltage signals from FSRs are transmitted to the laptop computer through the microcontroller unit (Arduino Uno). Artificial tissue made by Ecoflex[1] 00-30 is in a holder and attached to a reference force sensor (ATI Nano 17). Therefore, the force applied to tissue by the needle will be recorded via a PCI-6220 data acquisition board (National Instruments, USA) by the commercial sensor. The real-time monitoring and data acquisition of three voltage changes and 3-D interaction forces starts simultaneously at a frequency of 30 Hz.

Six groups of experiments with different insertion angles (0°, 15°, 30°, 45°, 60°, and 75°) are performed as shown in Fig. 6. Fig. 6(b) also shows the results of 3-D force information ($F_x = 0.3$ N, $F_y = 0.5$ N, and $F_z = 0.3$ N) when the needle is inserted at the maximum depth of the tissue. The coordinate of the tissue center is measured, and then we input the position coordinates and rotation angles of the end-effector into the robotic controller program. The insertion speed is set to 1 mm/s and lasts for 10 s. Then, the retraction speed is set to 2 mm/s until it finishes. For one insertion angle experiment, we will collect tens of thousands of valid data at different tissue points to eliminate the errors caused by inhomogeneous material properties.

V. Results

We evaluate our pretrained LS and FNN models with different insertion angles (0°, 15°, 30°, 45°, 60°, and 75°). For each insertion angle, an external dataset is used to further verify the reliability and efficacy of the models. Fig. 7 illustrates the selected 80-s interval of the typical force profile (30°) of insertion experiments to compare the performance of LS and FNN models. The predicted value of the LS model has a large difference between the reference values, especially the peak forces with a large time delay. The LS model has reverse predictions during the retraction process because the insertion process performs a larger weight on peak forces. It will cause the prediction of force to be the opposite. The FNN model can successfully predict the insertion force profiles despite small variations in peak points. Besides, the voltage outputs of the FSR can predict the pulling force as the start point of voltage is 0, because we embed the soft materials in the estimator design. For the initial state of the estimator, FSRs have been pressed and squeezed by soft materials. However, we can see the obvious fluctuations of predicted values over the reference forces in three directions. In Fig. 7, the puncture process can be divided into stage A (insertion) and stage B (retraction) based on captured 3-D force information. At the end of the retraction process, we note that the opposite resultant force can also be captured by the FNN model. This also proves that the design of the working area helps the feature capture in the experimental data-driven fitting.

The root mean squared error (RMSE) and normalized RMSE are used as evaluation metrics to test the performance of our proposed models (LS and FNN). The following formulas describe the calculation process:

$$\text{RMSE} = \sqrt{\frac{1}{N}\sum_{i=1}^{N}\left(\hat{f} - f\right)^2} \tag{3}$$

$$\text{NRMSE} = \frac{\text{RMSE}}{f_{\max} - f_{\min}} \times 100\% \tag{4}$$

where f is the predicted values and f represents the reference values. The results are shown in Table I. Due to the difference in angles, the magnitude of RMSE among X, Y, and Z forces can have large variations. In terms of the LS model, the average value of RMSE for six groups is 0.0928, 0.2689, and 0.4438 N. The corresponding average NRMSE values for the X-, Y-, Z-directions is 20.16%, 21.96%, 23.91%, respectively. For the FNN model, the average value of RMSE is 0.0383, 0.0098, and 0.1476 N for F_x, F_y, and F_z, respectively. Besides, the relative NRMSE for three directions is 8.34%, 8.11%, and 7.95%, respectively. Compared to the LS model, the accuracy of FNN is approximately two times higher than the LS model for any insertion degree. Therefore, we select the FNN model for the force estimation in the simulator.

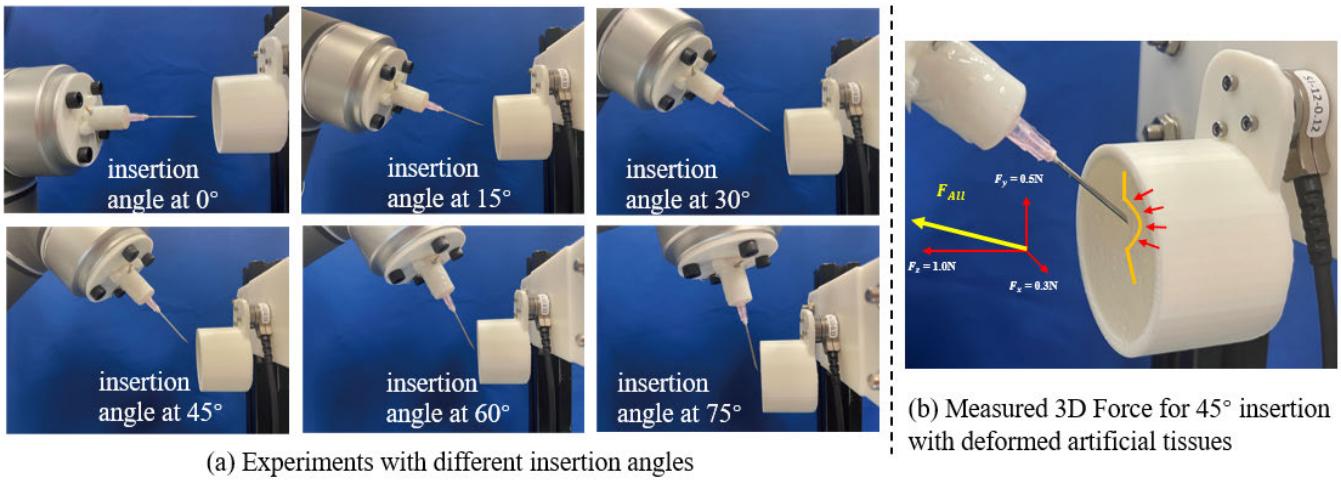

Fig. 6. Illustration of the experimental process. (a) Estimator is mounted on the UR5 robotic arm for insertion in different angles (0°, 15°, 30°, 45°, 60°, and 75°). (b) When the needle is inserted at the maximum depth of tissue, the 3-D force information is recorded.

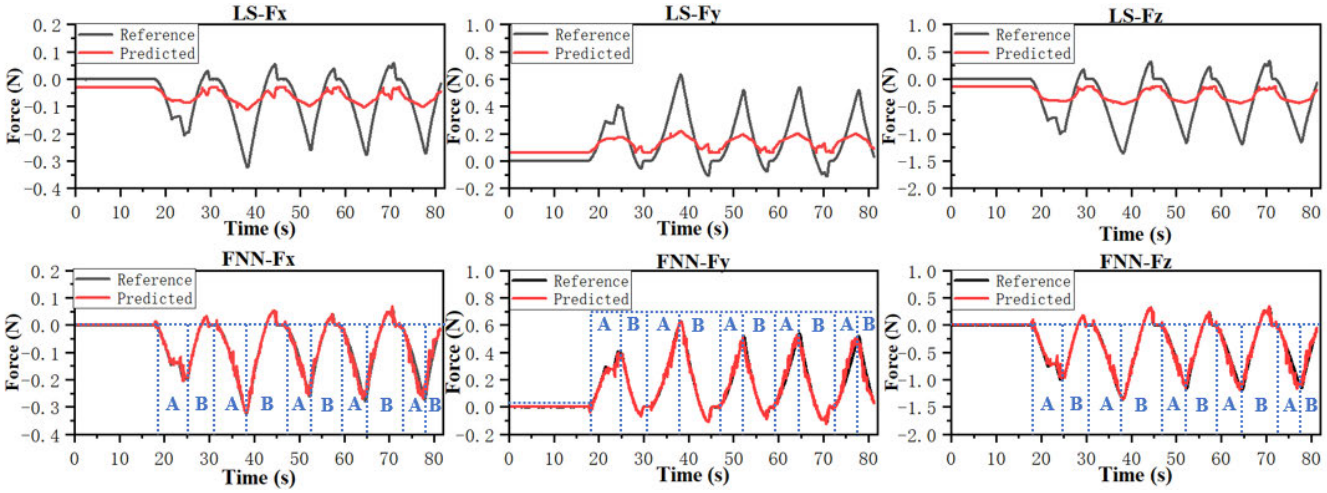

Fig. 7. Force profile of the FNN and LS model (30° insertion). A represents the insertion process and B is the retraction process.

TABLE I
COMPARISON OF THE LS METHOD AND THE FNN MODEL

Method	Evaluation metrics		
	NRMSE of Fx	NRMSE of Fy	NRMSE of Fz
LS (0°)	15.94%	14.14%	25.23%
FNN (0°)	9.92%	7.86%	7.35%
LS (15°)	19.03%	20.17%	21.43%
FNN (15°)	10.56%	10.29%	9.74%
LS (30°)	18.82%	21.50%	23.52%
FNN (30°)	4.84%	4.69%	4.48%
LS (45°)	17.76%	18.75%	20.57%
LS (45°)	7.18%	7.06%	7.18%
LS (60°)	24.61%	25.53%	23.54%
FNN (60°)	8.29%	9.42%	9.25%
LS (75°)	24.85%	31.72%	29.15%
FNN (75°)	7.62%	7.47%	7.20%

It can be seen that each insertion angle corresponds to the different well-trained FNN models. Therefore, a single insertion angle model with an acceptable covering range is crucial for practical application. For example, a 0° FNN model can have a reasonable error when fitting into the 15° insertion angle dataset. The results are presented in Table II. The RMSE and NRMSE of the 30° gap can be at 0.5024% and 40.06% at most for the Y-direction force prediction. The performance in the X- and Y-directions is not better than that of the average value of the previously presented LS model. Meanwhile, the average RMSE for the 15° difference dataset is 0.036, and NRMSE at 15.64%. From the force profile presented in Fig. 8, the results of 15° angle gap show that the fluctuations in the X-, Y-, and Z-directions are obvious. However, it can capture the shape of the force curve and predict the peak force. On the other hand, for the 30° gap dataset, predicted 3-D force information fails to match the overall trend of reference values and can have a large deviation from reference values. Therefore, in the training setting of a simulator, we can use the force information with different features to inform the trainee of the range of deviations from the standard insertion angle.

VI. DISCUSSION

In the research on needle puncture, the angle of entry becomes a significant issue in medical training. This factor directly affects the success rate of the puncture, the level

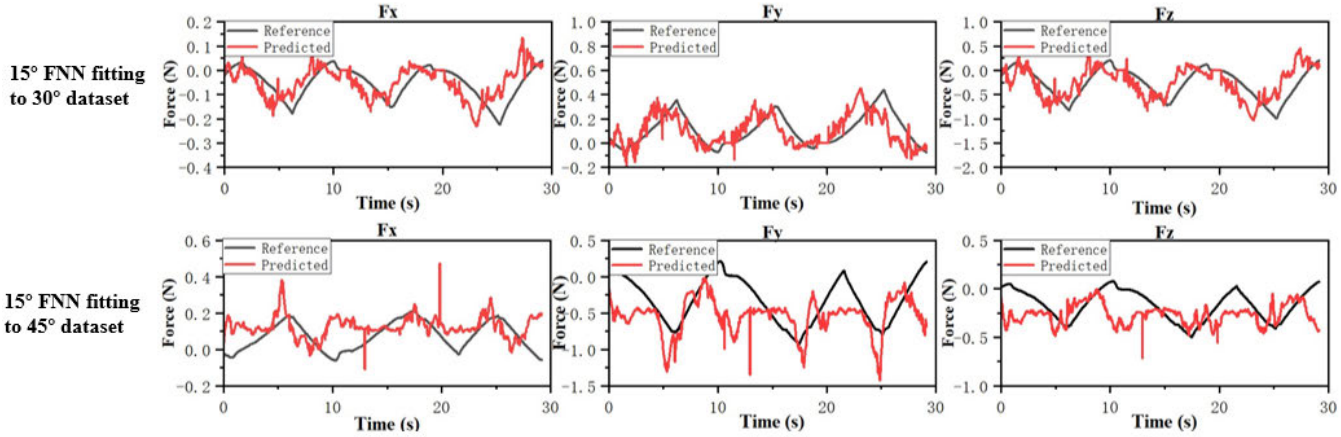

Fig. 8. Example of validation tests for different insertion angle gap (15° model fitting to the 30° dataset, 15° model fitting to 45° dataset).

TABLE II
COMPARISON OF FNN MODEL PERFORMANCE ON DIFFERENT ANGLE GAPS

Angle gap	Evaluation metrics		
	NRMSE of Fx	NRMSE of Fy	NRMSE of Fz
FNN (15°)	15.94%	14.14%	16.84%
FNN (30°)	30.24%	40.06%	35.56%

TABLE III
COMPARISON OF LSTM AND FNN NETWORKS

Method&Dataset	Evaluation metrics		
	NRMSE of Fx	NRMSE of Fy	NRMSE of Fz
LSTM (30°)	6.11%	5.80%	5.74%
FNN (30°)	**4.84%**	**4.69%**	**4.48%**
LSTM(angle gap 15°)	**14.38%**	**12.28%**	**14.14%**
FNN (angle gap 30°)	15.94%	14.14%	16.84%

of pain experienced by the patients, and the magnitude of tissue stress. Zhu et al. [28] discussed the optimal entry angle of the dorsal hand intravenous robot and claimed that a larger entry angle (60°) is preferred to reduce the pain of the patient. Therefore, the different entry angles have different force profiles. By comparing the force curve obtained through data-driven training with the actual force curve, we can determine the deviation range from the ideal angle (with a unit deviation of 15°). When the angle deviation is within 15°, it is possible to predict a force curve that remains consistent with the actual curve in terms of trend and magnitude. However, there may be a certain degree of time delay between the predicted and actual force curves. When the angle deviation reaches 30°, the model's failure becomes evident. Therefore, it can be considered as exceeding the predetermined angle range, requiring operators to make adjustments.

The presence of a 15° and 30° angle deviation allows for the prediction of a force curve that maintains consistency with the actual curve in terms of trend and magnitude, albeit with a certain degree of time delay. This is why it is used as a simulator cue. While the predicted force curve may introduce some error during actual operations due to the aforementioned angle deviation and time delay, the simulator serves as a valuable tool to assist operators in selecting suitable force application angles and anticipating potential deviations. By comparing the simulator's predictions with real-time data, operators can better comprehend and adjust their actions to achieve a closer approximation to the expected force application. These simulator cues provide more accurate references, aiding operators in optimizing their skills and performance.

Since our data is in the time domain, it is worth using an RNN, such as a long short-term memory (LSTM), to predict the 3-D force profiles. To compare the performance of LSTM networks, we selected two datasets: one with a needle insertion angle of 30° and another where we fit the data with a 15° deviation to represent a 30° angle gap. From Table III, it can be observed that the FNN outperformed the LSTM on the dataset without angle deviation. For the prediction of force in the X-, Y-, and Z-directions, the FNN achieved an average NRMSE of 4.67%, while the LSTM had an NRMSE of 5.88%. On the dataset with angle deviation (15°), it can be observed that the LSTM outperformed the FNN. The corresponding average NRMSE values were 13.6% for the LSTM and 15.64% for the FNN. For the FNN, it performs better on datasets with more regular patterns, such as the one without angle deviation. The LSTM is well-suited for fitting time-domain data, and it can handle fluctuations and outliers present in the dataset with angle deviation. The LSTM can capture trends and patterns to predict the next point, thereby reducing errors. It is necessary to clarify that our objective is to provide 3-D tactile cues for needle insertion. Our primary criterion for selecting the network is to make the cues more suitable for the scenario at hand. For the dataset without angle deviation, we choose the FNN because, in this scenario, the cues aim to assist the operator in maintaining a stable needle insertion angle. For the dataset with angle deviation, we need to provide cues to indicate when the operator is at the incorrect angle. In this case, having some errors can be helpful for the cues. However, the presence of outliers at certain points can lead to incorrect cues, such as indicating a 30° deviation instead of the actual 15° deviation. Then, the LSTM can be an alternative when performing angle deviation cues.

VII. Conclusion

Needle insertion tasks for different medical applications are in high demand. Providing a low-cost simulator with adequate guidance and feedback is crucial for large-scale deployment when the workforce is insufficient. From the fabrication perspective, the miniaturization and integrated manufacturing of force-sensing systems are significant challenges for various applications. Besides, capturing X-, Y-, and Z-direction forces and reducing the cost of 3-D force estimators are two problems in practical application. This article proposes a new fabrication method costing less than 5 USD and data-driven estimators to obtain 3-D force profiles toward the needle insertion simulator. A 14-mm triaxial force estimator with an FNN neural network model can achieve above 90% data fitting accuracy in RMSE for each insertion angle. On the contrary, the LS has a lower average accuracy of 80%. The reflection on the graph of the LS method shows that it can only present the trend of force for the reference value but with large differences in the numerical values, especially the static force at 0 N and the peak force during the insertion process. Therefore, the FNN model has selected tests with angle gaps. We use the selected single insertion angle model to test the validity to different ranges and prove that $\pm 15^\circ$ can have above 85% accuracy. The obvious fluctuations are presented in the curve, but it can capture the overall trend and the peak force value. For the test on $\pm 30^\circ$, the randomness of the curve and the unexpected outlier make such an angle gap unsuitable for practical application. Therefore, we can summarize the functions of force estimators in the simulator as follows.

1) If the trainee is at the preset correct insertion angle with the appropriate force magnitude, the simulator will inform the user to continue as the estimated force profiles match the reference values.
2) If the insertion angle has deviations from the preset one, the simulator will warn or inform the user to stop or correct based on the predicted features of force profiles.

In the future, we expect validation tests on trainees and to obtain user experience feedback with the user application to be developed.

Acknowledgment

Ruijie Tang and Long Bai are with the Department of Electronic Engineering, The Chinese University of Hong Kong, Hong Kong, China (e-mail: ruijie.tang@link.cuhk.edu.hk; b.long@ieee.org).

Shilong Yao is with the Department of Electrical Engineering, City University of Hong Kong, Hong Kong, China, also with the Shenzhen Key Laboratory of Robotics Perception and Intelligence, Shenzhen 518055, China, and also with the Department of Electronic and Electrical Engineering, Southern University of Science and Technology, Shenzhen 518055, China (e-mail: shilong.yao@my.cityu.edu.hk).

Hong Yan is with the Department of Electrical Engineering, City University of Hong Kong, Hong Kong, China (e-mail: h.yan@cityu.edu.hk).

Max Q.-H. Meng is with the Shenzhen Key Laboratory of Robotics Perception and Intelligence, Shenzhen 518055, China, and also with the Department of Electronic and Electrical Engineering, Southern University of Science and Technology, Shenzhen 518055, China (e-mail: max.meng@ieee.org).

Hongliang Ren is with the Department of Electronic Engineering, Shun Hing Institute of Advanced Engineering, The Chinese University of Hong Kong, Hong Kong, China, also with the Department of Biomedical Engineering, National University of Singapore (NUS), Singapore 117575, and also with NUS (Suzhou) Research Institute, Suzhou 215123, China (e-mail: hlren@ieee.org).

References

[1] L. T. Kohn, J. M. Corrigan, and M. S. Donaldson, "Errors in health care: A leading cause of death and injury," in *To Err is Human: Building a Safer Health System*. Washington, DC, USA: National Academies Press, 2000.

[2] Y. Wu et al., "Transformer-based 3D U-Net for pulmonary vessel segmentation and artery-vein separation from CT images," *Med. Biol. Eng. Comput.*, vol. 61, no. 10, pp. 2649–2663, Oct. 2023.

[3] L. Bai, M. Islam, L. Seenivasan, and H. Ren, "Surgical-VQLA: Transformer with gated vision-language embedding for visual question localized-answering in robotic surgery," 2023, *arXiv:2305.11692*.

[4] L. Bai, M. Islam, and H. Ren, "Revisiting distillation for continual learning on visual question localized-answering in robotic surgery," 2023, *arXiv:2307.12045*.

[5] E. Nouvellon, P. Cuvillon, J. Ripart, and B. Riou, "Regional anesthesia and eye surgery," *Anesthesiology*, vol. 113, no. 5, pp. 1236–1242, Nov. 2010.

[6] A. G. Little, P. C. Kremser, J. L. Wade, J. M. Levett, T. R. DeMeester, and D. B. Skinner, "Operation for diagnosis and treatment of pericardial effusions," *Surgery*, vol. 96, no. 4, pp. 738–744, 1984.

[7] S. H. Parker, A. T. Stavros, and M. A. Dennis, "Needle biopsy techniques," *Radiologic Clinics North Amer.*, vol. 33, no. 6, pp. 1171–1186, 1995.

[8] A. Delaney, S. M. Bagshaw, and M. Nalos, "Percutaneous dilatational tracheostomy versus surgical tracheostomy in critically ill patients: A systematic review and meta-analysis," *Crit. Care*, vol. 10, no. 2, pp. 1–13, 2006.

[9] X. Xiao et al., "Portable body-attached positioning mechanism toward robotic needle intervention," *IEEE/ASME Trans. Mechatronics*, vol. 25, no. 2, pp. 1105–1116, Apr. 2020.

[10] J. Y. Lee et al., "Ultrasound needle segmentation and trajectory prediction using excitation network," *Int. J. Comput. Assist. Radiol. Surg.*, vol. 15, no. 3, pp. 437–443, Mar. 2020.

[11] Z. Zhao, S. Xu, B. J. Wood, H. Ren, and Z. T. H. Tse, "The feasibility of using a smartphone magnetometer for assisting needle placement," *Ann. Biomed. Eng.*, vol. 48, no. 4, pp. 1147–1156, Apr. 2020.

[12] H. Gao, X. Xiao, L. Qiu, M. Q.-H. Meng, N. K. K. King, and H. Ren, "Remote-center-of-motion recommendation toward brain needle intervention using deep reinforcement learning," in *Proc. IEEE Int. Conf. Robot. Autom. (ICRA)*, May 2021, pp. 8295–8301.

[13] D. J. van Gerwen, J. Dankelman, and J. J. van den Dobbelsteen, "Needle-tissue interaction forces—A survey of experimental data," *Med. Eng. Phys.*, vol. 34, no. 6, pp. 665–680, Jul. 2012.

[14] B. Maurin et al., "In vivo study of forces during needle insertions," in *Perspective in Image-Guided Surgery*. Singapore: World Scientific, 2004, pp. 415–422.

[15] T. Lehmann, M. Tavakoli, N. Usmani, and R. Sloboda, "Force-sensor-based estimation of needle tip deflection in brachytherapy," *J. Sensors*, vol. 2013, pp. 1–10, Jun. 2013.

[16] L. Barbé, B. Bayle, M. de Mathelin, and A. Gangi, "Needle insertions modeling: Identifiability and limitations," *Biomed. Signal Process. Control*, vol. 2, no. 3, pp. 191–198, Jul. 2007.

[17] J. T. Hing, A. D. Brooks, and J. P. Desai, "Reality-based needle insertion simulation for haptic feedback in prostate brachytherapy," in *Proc. IEEE Int. Conf. Robot. Autom.*, May 2006, pp. 619–624.

[18] J. Zhai et al., "A sensor for needle puncture force measurement during interventional radiological procedures," *Med. Eng. Phys.*, vol. 35, no. 3, pp. 350–356, Mar. 2013.

[19] P. Puangmali, K. Althoefer, L. D. Seneviratne, D. Murphy, and P. Dasgupta, "State-of-the-art in force and tactile sensing for minimally invasive surgery," *IEEE Sensors J.*, vol. 8, no. 4, pp. 371–381, Apr. 2008.

[20] A. Gijbels, E. B. V. Poorten, P. Stalmans, and D. Reynaerts, "Development and experimental validation of a force sensing needle for robotically assisted retinal vein cannulations," in *Proc. IEEE Int. Conf. Robot. Autom. (ICRA)*, May 2015, pp. 2270–2276.

[21] Y. Noh, S. Han, P. Gawenda, W. Li, S. Sareh, and K. Rhode, "A contact force sensor based on S-shaped beams and optoelectronic sensors for flexible manipulators for minimally invasive surgery (MIS)," *IEEE Sensors J.*, vol. 20, no. 7, pp. 3487–3495, Apr. 2020.

[22] S. Sefati, C. Gao, I. Iordachita, R. H. Taylor, and M. Armand, "Data-driven shape sensing of a surgical continuum manipulator using an uncalibrated fiber Bragg grating sensor," *IEEE Sensors J.*, vol. 21, no. 3, pp. 3066–3076, Feb. 2021.

[23] Y. Ma, X. Xiao, H. Ren, and M. Q.-H. Meng, "A review of bio-inspired needle for percutaneous interventions," *Biomimetic Intell. Robot.*, vol. 2, no. 4, Dec. 2022, Art. no. 100064.

[24] D. Kim and Y.-L. Park, "Contact localization and force estimation of soft tactile sensors using artificial intelligence," in *Proc. IEEE/RSJ Int. Conf. Intell. Robots Syst. (IROS)*, Oct. Oct. 2018, pp. 7480–7485.
[25] J. Hu, J. Back, P. Dasgupta, and H. Liu, "Embedding soft material channels for tactile sensing of complex surfaces—Mathematical modeling," *IEEE Sensors J.*, vol. 21, no. 3, pp. 3172–3183, Feb. 2021.
[26] J. Y. Loo, Z. Y. Ding, V. M. Baskaran, S. G. Nurzaman, and C. P. Tan, "Robust multimodal indirect sensing for soft robots via neural network-aided filter-based estimation," *Soft Robot.*, vol. 9, no. 3, pp. 591–612, Jun. 2022.
[27] R. Tang, J. Zheng, and S. Wang, "Design of novel end-effectors for robot-assisted swab sampling to combat respiratory infectious diseases," in *Proc. 43rd Annu. Int. Conf. IEEE Eng. Med. Biol. Soc. (EMBC)*, Nov. 2021, pp. 4757–4760.
[28] Z. Zhu, K. Li, G. Zhang, H. Jin, Z. Zhu, and P. Wang, "Decision method of optimal needle insertion angle for dorsal hand intravenous robot," *Sensors*, vol. 23, no. 2, p. 848, Jan. 2023.

Ruijie Tang received the dual B.S. degree in mechanical engineering from the South China University of Technology, Guangzhou, China, and The University of Edinburgh, Edinburgh, U.K., in 2018, and the M.S. degree in advanced aeronautical engineering, Imperial College London, London, U.K., in 2019. He is currently pursuing the Ph.D. degree in electronic engineering, The Chinese University of Hong Kong, Hong Kong.

His current research interests include soft robots, force sensor design, and magnetically actuated robots with applications in the medical field.

Shilong Yao received the B.E. degree in mechanical engineering from the Southern University of Science and Technology, Shenzhen, China, in 2021. He is currently pursuing the Ph.D. degree with the Department of Electrical Engineering, City University of Hong Kong (CityU), Hong Kong.

His current research interests include surgical robotic systems and machine learning in medical robotics.

Long Bai (Graduate Student Member, IEEE) received the B.S. degree in optoelectronics information science and engineering from the Beijing Institute of Technology (BIT), Beijing, China, in 2021. He is currently pursuing the Ph.D. degree with the Department of Electronic Engineering, The Chinese University of Hong Kong (CUHK), Hong Kong.

His current research interests include robotics perception, capsule endoscopy, surgical scene understanding, continual learning, and human–robot interaction.

Mr. Bai was a recipient of the CUHK Vice-Chancellor's Ph.D. Scholarship Scheme in 2021, the IEEE RAS Travel Grants Award in 2023, the Best Poster Award in ICRA Workshop on Surgical Robotics in 2023, and the ICBIR Best Student Paper Award in 2023.

Hong Yan (Fellow, IEEE) received the Ph.D. degree from Yale University, New Haven, CT, USA, in 1989.

He was a Professor of Imaging Science with The University of Sydney, Camperdown, Australia. Currently, he is a Wong Chun Hong Professor of Data Engineering and a Chair Professor of Computer Engineering with the City University of Hong Kong, Hong Kong. He has authored or coauthored over 600 journal and conference papers in these areas. His research interests include image processing, pattern recognition, and bioinformatics.

Dr. Yan is an IAPR Fellow, a member of the European Academy of Sciences and Arts, and a Fellow of the US National Academy of Inventors. He received the 2016 Norbert Wiener Award for contributions to image and biomolecular pattern recognition techniques from the IEEE SMC Society.

Max Q.-H. Meng (Fellow, IEEE) received the Ph.D. degree in electrical and computer engineering from the University of Victoria, Victoria, BC, Canada, in 1992.

He is currently a Chair Professor and the Head of the Department of Electronic and Electrical Engineering with the Southern University of Science and Technology, Shenzhen, China, on leave from the Department of Electronic Engineering, The Chinese University of Hong Kong, Hong Kong. He joined The Chinese University of Hong Kong as a Professor in 2001 and later the Chairperson of the Department of Electronic Engineering. He was with the Department of Electrical and Computer Engineering, University of Alberta, Edmonton, AB, Canada, where he was the Director of the Advanced Robotics and Teleoperation Laboratory and held the positions of assistant professor in 1994, an Associate Professor in 1998, and a Professor in 2000. He has authored or coauthored more than 750 journal and conference papers and book chapters and led more than 60 funded research projects to completion as a Principal Investigator. His research interests include robotics, perception, and intelligence.

Prof. Meng is an Elected Member of AdCom of IEEE RAS for two terms. He is a Fellow of the Hong Kong Institution of Engineers and an Academician of the Canadian Academy of Engineering. He was a recipient of the IEEE Millennium Medal. He is the General Chair or the Program Chair of many international conferences, including the General Chair of IROS 2005 and ICRA 2021, respectively. He served as an Associate VP for Conferences of the IEEE Robotics and Automation Society from 2004 to 2007 and the Co-Chair of the Fellow Evaluation Committee. He is the Editor-in-Chief and an Editorial Board for a number of international journals, including the Editor-in-Chief for the *Biomimetic Intelligence and Robotics* (Elsevier).

Hongliang Ren (Senior Member, IEEE) received the Ph.D. degree in electronic engineering (specializing in biomedical engineering) from The Chinese University of Hong Kong (CUHK), Hong Kong, in 2008.

He has navigated his academic journey through CUHK, Johns Hopkins University, Baltimore, MD, USA, the Children's Hospital Boston, Boston, MA, USA, the Harvard Medical School, Boston, Children's National Medical Center, Washington, DC, USA, and the National University of Singapore (NUS), Singapore. He is currently an Associate Professor with the Department of Electronic Engineering, CUHK, and an Adjunct Associate Professor with the Department of Biomedical Engineering, NUS. His research interests include biorobotics, intelligent control, medical mechatronics, soft continuum robots, soft sensors, and multisensory learning in medical robotics.

Dr. Ren was a recipient of the NUS Young Investigator Award, the Engineering Young Researcher Award, the IAMBE Early Career Award 2018, the Interstellar Early Career Investigator Award 2018, the ICBHI Young Investigator Award 2019, and the Health Longevity Catalyst Award (2022 by NAM & RGC). He has served as an Associate Editor for IEEE TRANSACTIONS ON AUTOMATION SCIENCE AND ENGINEERING and *Medical & Biological Engineering & Computing (MBEC)*.